



An *in vitro* model for microbial fructoselysine degradation shows substantial interindividual differences in metabolic capacities of human fecal slurries

Katja C.W. van Dongen^{a,*}, Meike van der Zande^b, Ben Bruyneel^a, Jacques J.M. Vervoort^c,
Ivonne M.C.M. Rietjens^a, Clara Belzer^d, Karsten Beekmann^{a,b}

^a Division of Toxicology, Wageningen University and Research, P.O. Box 8000, 6700 EA Wageningen, the Netherlands

^b Wageningen Food Safety Research (WFSR), part of Wageningen University and Research, P.O. Box 230, 6700 AE Wageningen, the Netherlands

^c Laboratory of Biochemistry, Wageningen University and Research, P.O. Box 8128, 6700 ET Wageningen, the Netherlands

^d Laboratory of Microbiology, Wageningen University and Research, P.O. Box 8033, 6700 EH Wageningen, the Netherlands

ARTICLE INFO

Keywords:

Amadori product
Human gut microbiota
Interindividual differences
Michaelis-Menten kinetics
Short chain fatty acid (SCFA)

ABSTRACT

Fructoselysine is formed upon heating during processing of food products, and being a key intermediate in advanced glycation end product formation considered to be potentially hazardous to human health. Human gut microbes can degrade fructoselysine to yield the short chain fatty acid butyrate. However, quantitative information on these biochemical reactions is lacking, and interindividual differences therein are not well established. Anaerobic incubations with pooled and individual human fecal slurries were optimized and applied to derive quantitative kinetic information for these biochemical reactions. Of 16 individuals tested, 11 were fructoselysine metabolizers, with V_{max} , K_m and k_{cat} -values varying up to 14.6-fold, 9.5-fold, and 4.4-fold, respectively. Following fructoselysine exposure, 10 of these 11 metabolizers produced significantly increased butyrate concentrations, varying up to 8.6-fold. Bacterial taxonomic profiling of the fecal samples revealed differential abundant taxa for these reactions (e.g. families *Ruminococcaceae*, *Christenellaceae*), and *Ruminococcus_1* showed the strongest correlation with fructoselysine degradation and butyrate production ($\rho \geq 0.8$).

This study highlights substantial interindividual differences in gut microbial degradation of fructoselysine. The presented method allows for quantification of gut microbial degradation kinetics for foodborne xenobiotics, and interindividual differences therein, which can be used to refine prediction of internal exposure.

1. Introduction

Fructoselysine is the most abundant Amadori product in food products and is formed during heating in the processing and preparation of food products (Erbersdobler and Faist, 2001). Fructoselysine is formed via the Maillard reaction by a non-enzymatic reaction between a reducing sugar (i.e. glucose) and the amino group of protein-bound or free lysine (Yaylayan et al., 1994), as depicted in Fig. 1. It occurs in a variety of food products, such as baked products, fried potatoes and infant formula (Erbersdobler and Somoza, 2007; Mehta and Deeth, 2016), with a total daily intake in the Western diet reported to be

500–1000 mg free and protein-bound fructoselysine (corresponding to 7.1–14.3 mg/kg bw/day for a 70 kg adult) (Hellwig et al., 2015). The presence of fructoselysine in food raises a concern, as it is a key intermediate in the formation of advanced glycation end products (AGEs) such as carboxymethyllysine (Ahmed et al., 1986). Also, fragmentation of fructoselysine can result in formation of reactive α -dicarbonyls (i.e. glyoxal, 3-deoxyglucosone) (Brings et al., 2017; Henle, 2005; Yaylayan et al., 1994) which, in turn, can form new (protein-bound) AGEs (Koschinsky et al., 1997; Van Nguyen, 2006). AGEs have been associated with several (chronic) diseases and inflammation, such as the development of atherosclerosis, the onset of diabetes complications, and Crohn's

Abbreviations: ¹³C-3NPH-HCl, ¹³C₆-3-nitrophenylhydrazine hydrochloride; 3NPH-HCl, 3-nitrophenylhydrazine hydrochloride; ADME, absorption distribution metabolism excretion; AGE, advanced glycation end-product; CE, collision energy; EDC, N-(3-dimethylaminopropyl)-N'-ethylcarbodiimide; IS-SCFA, ¹³C isotope labelled derivatized SCFA standard; ISTD, internal standard; k_{cat} , catalytic efficiency; K_m , Michaelis-Menten constant; LDA, linear discriminant analysis; LEfSe, LDA effect size; MRM, multiple reaction monitoring; OTU, operational taxonomic unit; PERMANOVA, permutational multivariate analysis of variance; PBK, physiologically based kinetic; RAGE, receptor for advanced glycation end products; V_{max} , maximum velocity.

* Corresponding author at: Division of Toxicology, Wageningen University, P.O. Box 8000, 6700 EA Wageningen, the Netherlands.

E-mail address: katja.vandongen@wur.nl (K.C.W. van Dongen).

<https://doi.org/10.1016/j.tiv.2021.105078>

Received 5 November 2020; Accepted 5 January 2021

Available online 8 January 2021

0887-2333/© 2021 The Authors.

Published by Elsevier Ltd.

This is an open access article under the CC BY-NC-ND license

(<http://creativecommons.org/licenses/by-nc-nd/4.0/>).

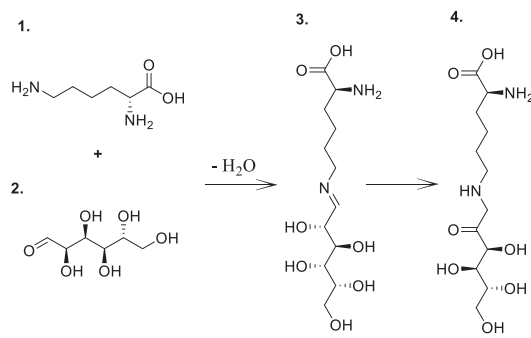


Fig. 1. Fructoselysine (4) formation via reaction between the ϵ -amino moiety of lysine (1) and glucose (2), to form the so-called Schiff base (3), which subsequently undergoes an Amadori rearrangement reaction to yield fructoselysine (4).

disease (Ciccocioppo et al., 2013; Delgado-Andrade and Fogliano, 2018; Kellow and Coughlan, 2015; Poulsen et al., 2013; Sergi et al., 2020). Both free- and protein-bound AGEs can cause oxidative stress (Liu et al., 2016), and glycation of proteins can alter their structure and function, in addition to turning them into agonists for the receptor for AGEs (RAGE) which, upon activation, exerts pro-inflammatory responses (Delgado-Andrade and Fogliano, 2018; Uribarri et al., 2005). While the interactions with RAGE appear to occur mainly if not only with AGEs bound to high molecular weight proteins (Kislinger et al., 1999; Xue et al., 2011), there is currently no consensus on which biological effects can be attributed to free AGEs or AGEs bound to low molecular weight proteins (Zhao et al., 2019). While endogenously formed AGEs are certainly an important source of internal AGE exposure, AGEs present in food contribute significantly to the endogenous AGE pool, both in plasma and tissues (Koschinsky et al., 1997; Li et al., 2015; Scheijen et al., 2018; Uribarri et al., 2005; Vlassara and Palace, 2002). A dose-dependent increase of fructoselysine has been reported in plasma, liver and kidney resulting from dietary, protein-bound fructoselysine exposure in experimental animals (Somoza et al., 2006). It is also reported that fructoselysine and several free or (peptide)bound AGEs can reach the colon as they have a low (systemic) bioavailability (Liang et al., 2019). Free fructoselysine is transported, albeit poorly, via simple diffusion over Caco-2 monolayers in vitro (Grunwald et al., 2006) and dipeptide bound fructoselysine partially via the peptide transporter PEPT1 (Hellwig et al., 2011). In human volunteers fed a meal rich in protein-bound fructoselysine, only $\pm 3\%$ of ingested fructoselysine was excreted in urine, and only $\pm 1\%$ recovered in feces, implying a high degree of metabolism (Erbersdobler and Faist, 2001; Lee and Erbersdobler, 2005). Together, this suggests that colonic microbiota metabolize the majority of ingested fructoselysine (Erbersdobler and Faist, 2001; Snelson and Coughlan, 2019). This is supported by in vitro incubations with human fecal samples (Hellwig et al., 2015) which show that the intestinal microbiota can metabolize fructoselysine, in addition to few specific isolated bacterial strains which are reported to be able to degrade fructoselysine, i.e. *Escherichia coli* (Wiame et al., 2002), *Bacillus subtilis* (Wiame et al., 2004), and *Intestinimonas butyriciproducens* AF211 (Bui et al., 2015). *I. butyriciproducens* AF211, isolated from human feces, was also shown to produce the short chain fatty acid (SCFA) butyrate from fructoselysine (Bui et al., 2015). Butyrate, together with acetate and propionate represent the major SCFAs in the colon (den Besten et al., 2013). These gut microbial fermentation products have several important functions for (intestinal) host health (den Besten et al., 2013; Hamer et al., 2007; Nicholson et al., 2012), implying that fructoselysine might be converted by gut bacteria into beneficial metabolites. However, only $\pm 10\%$ of 65 fecal samples in the Human Microbiome Project contained *I. butyriciproducens* AF211 genes in the deep metagenome (Bui et al., 2015; Huttenhower et al., 2012), and the other bacteria identified might only be capable of performing certain steps in this complex process,

suggesting the potential existence of interindividual differences. To date, no data on the catalytic efficiencies, and interindividual differences in gut microbial fructoselysine degradation, along with SCFA formation have been reported. In this study, an in vitro method was optimized and applied to derive the catalytic efficiency of fructoselysine degradation and accompanying SCFA production, to quantify interindividual differences therein, and to investigate associations with bacterial composition based on 16S rRNA gene sequencing.

2. Materials and methods

2.1. Chemicals and reagents

Fructoselysine (CAS: 21291-40-7) was purchased from Carbosynth Limited (Berkshire, UK). 3-Nitrophenylhydrazine hydrochloride (3NPH-HCl; CAS: 636-95-3), N-(3-dimethylaminopropyl)-N'-ethylcarbodiimide (EDC; CAS: 25952-53-8), pyridine anhydrous (CAS: 110-86-1), glycerol (CAS: 56-81-5), sodium propionate (CAS: 137-40-6) and sodium butyrate (CAS: 156-54-7) were purchased from Sigma-Aldrich (Steinheim, Germany). Formic acid (99-100%, analytical grade; CAS: 64-18-6) and sodium acetate anhydrous (CAS: 127-09-3) were purchased from Merck (Darmstadt, Germany). $^{13}\text{C}_6$ -3-nitrophenylhydrazine hydrochloride (^{13}C -3NPH-HCl; CAS: 1977535-33-3) was obtained from Cayman Chemicals (Ann Arbor, USA). PBS was purchased from Gibco (Paisley, UK). Acetonitrile (ACN; UPLC/MS grade; CAS: 75-05-8) was obtained from BioSolve BV (Valkenswaard, the Netherlands).

2.2. Collection of human fecal samples

Fresh fecal samples were collected from 16 human individual volunteers (12 females, 4 males) aged between 24 and 64 years of Caucasian, Asian, and Hispanic demographic origin. Volunteers were not pregnant, did not suffer from chronic gastrointestinal diseases and did not use antibiotics three months prior to donation. Fecal samples were collected fresh in fecal collection tubes and were immediately processed in an anaerobic environment (85% CO_2 , 5% H_2 , 10% N_2). After a four times dilution (w/v) in anaerobic storage buffer (10% glycerol in PBS), samples were filtered using a SpinCon system (Meridian Bioscience), which was centrifuged for 5 min at 3000 $\times g$ at 10 $^\circ\text{C}$. After filtration, samples were homogenized before aliquots were prepared and stored at $-80\text{ }^\circ\text{C}$ until further use.

This study was assessed by the Medical Ethical Committee of Wageningen University and judged to not fall under the Dutch 'Medical Research Involving Human Subjects Act'. Participants granted informed consent before participation in this study.

2.3. Incubations of the fecal slurries with fructoselysine

All fecal incubations were performed under anaerobic conditions at 37 $^\circ\text{C}$. Experimental conditions were optimized by assessing linearity of fructoselysine degradation over time and over the amount of pooled fecal slurry, which consisted of equal amounts of the 16 individual fecal samples. 40 μM fructoselysine was incubated with 2.5%, 5% or 10% pooled fecal slurry in anaerobic PBS, in a volume of 50 μL per Eppendorf tube in technical triplicates for 0, 20, 40, 60 and 80 min. 5% Fecal slurry, corresponding to 0.0125 g feces/mL, and an incubation time of 60 min were selected for further experiments to derive Michaelis-Menten kinetics of fructoselysine degradation of both pooled and individual human fecal slurries. These were incubated in technical duplicates with increasing fructoselysine concentrations ranging from 0 to 400 μM for the pooled and 0–600 μM for the individual incubations (added from 50 times concentrated aqueous stock solutions). These exposure concentrations cover the range of physiological relevant fructoselysine concentrations (81–162 μM) reached by the reported daily intake, taking into account the volume of the colon and the dilutions applied in the anaerobic incubations. For detection of SCFA formation, pooled or

individual fecal slurries (5%) were incubated in technical triplicates with a final concentration of 400 μM or 600 μM fructoselysine, respectively, in parallel to the solvent control. To terminate the reactions and to precipitate proteins, particles, and microorganisms 50 μL cold ACN (1:1) were added to the incubations. The remaining mixture was vortexed, stored on ice for at least 15 min, and centrifuged for 15 min at 18,000 $\times g$ at 4 °C. Supernatants were further processed for fructoselysine or SCFA measurement as described below. All incubations as described above were performed 3 times.

2.4. Fructoselysine measurement

The supernatants of the incubation samples were transferred to UPLC vials and analyzed by LC-MS/MS for fructoselysine quantification using a Shimadzu Nexera XR LC-20AD SR UPLC system coupled to a Shimadzu LCMS-8040 triple quadrupole MS (Kyoto, Japan). 2 μL supernatant were injected onto a Phenomenex Polar-RP Synergi column (30 \times 2 mm, 2.5 μm) at 40 °C. The mobile phase consisted of a gradient made from ultrapure water with 0.1% (v/v) formic acid and ACN with 0.1% (v/v) formic acid at a flow rate of 0.3 mL/min. The gradient started with 95% ACN for 2.5 min, to reach 0% ACN at 4 min, and was subsequently kept at 0% ACN until 6 min, followed by a shift to 100% ACN from 6 to 7.8 min returning to 95% ACN at 8.1 min and kept at these initial conditions up to 14 min. Under these conditions fructoselysine eluted at 5.6 min. The LCMS-8040 coupled with an ESI source was used for MS/MS identification. Positive ionization for multiple reaction monitoring (MRM) mode was used. Fructoselysine was quantified using precursor to product transition m/z 309.2 \rightarrow 84.2 (collision energy (CE) = -31 V) which was the most intense fragment ion. MRM transitions m/z 309.2 \rightarrow 291.1 (CE = -11 V), m/z 309.2 \rightarrow 273.1 (CE = -15 V) and m/z 309.2 \rightarrow 225.2 (CE = -17 V) were used as reference ions. An external calibration curve in matrix was prepared using a commercially available standard. Peak areas were integrated using LabSolutions software (Shimadzu). The amount of fructoselysine degraded during incubation was calculated and expressed in $\mu\text{mol/h/g}$ feces.

2.5. SCFA measurement

SCFAs in the supernatants of the incubation samples were derivatized and subsequently measured by LC-MS/MS, based on a previously described method with minor adaptations (Han et al., 2015). In short, 40 μL of the supernatant was mixed with freshly prepared 20 μL 200 mM 3NPH-HCl in 50% ACN and 20 μL 120 mM EDC-6% pyridine in 50% aqueous ACN solution in small glass tubes. After mixing, the tubes were placed with a cap in a 40 °C heating block and incubated for 30 min and afterwards placed on ice for 1 min. The mixture was diluted with 320 μL nanopure water. To 90 μL of this diluted mixture, 10 μL of ^{13}C isotope labelled derivatized SCFA standard mix (IS-SCFA mix) (prepared as described below) was added as internal standard (ISTD) to account for analytical variability. The IS-SCFA mix was created by using ^{13}C -3NPH-HCl instead of 3NPH-HCl and a mixture of the SCFAs acetate, propionate and butyrate resulting in final concentrations after derivatization of 500 μM , 400 μM and 400 μM , respectively. Further steps for the derivatization procedure were similar as described above. After the reaction, this IS-SCFA mix was aliquoted and stored at -80 °C in glass vials until use.

For quantification of the SCFAs, a calibration curve was prepared by derivatizing a concentration range of a mixture of acetate, propionate and butyrate with the same procedure as described above. To 90 μL of these derivatized SCFA standards, 10 μL of the IS-SCFA mix were added which resulted in a final concentration of 50 μM for acetate- ^{13}C -3NPH and 40 μM for propionate- ^{13}C -3NPH and butyrate- ^{13}C -3NPH.

A Shimadzu Nexera XR LC-20AD XR UPLC system coupled to a Shimadzu LCMS-8045 triple quadrupole mass spectrometer (Kyoto, Japan) was used for analysis of the SCFAs. 10 μL of sample were injected onto a Phenomenex Kinetex C18 column (50 \times 2.1 mm, 1.7 μm) at 40 °C.

The mobile phase consisted of a gradient made from ultrapure water with 0.1% (v/v) formic acid and ACN with 0.1% (v/v) formic acid at a flow rate of 0.6 mL/min. The gradient started with 10% ACN to reach 20% ACN at 4 min, followed by a shift to 100% ACN reached at 4.1 min, and was subsequently kept at 100% ACN until 7.5 min, returning to 10% ACN at 7.6 min and kept at these initial conditions up to 10 min. Under these conditions, acetate-3NPH and its ISTD acetate- ^{13}C -3NPH eluted at 1.3 min, propionate-3NPH and its ISTD propionate- ^{13}C -3NPH eluted at 2.3 min and butyrate-3NPH and its ISTD butyrate- ^{13}C -3NPH at 3.9 min. The LCMS-8045 was equipped with an ESI source and used for MRM quantification in negative ion mode. The following MRM transitions from precursor to product per compound were selected for quantification: acetate-3NPH m/z 194.0 \rightarrow 137.1 (CE = 17.0 V), acetate- ^{13}C -3NPH m/z 200.1 \rightarrow 143.1 (CE = 17.0 V), propionate-3NPH m/z 208.1 \rightarrow 137.1 (CE = 19.0 V), propionate- ^{13}C -3NPH m/z 214.1 \rightarrow 143.1 (CE = 19.0 V), butyrate-3NPH m/z 222.1 \rightarrow 137.1 (CE = 19.0 V) and butyrate- ^{13}C -3NPH m/z 228.1 \rightarrow 143.1 (CE = 19.0 V). The ratio of peak area in the unknown sample was divided by the peak area of the corresponding ISTD was used for quantification using the constructed calibration curve with ISTD IS-SCFA mix.

2.6. DNA isolation, PCR amplification of the 16S rRNA gene and sequencing

DNA from the fecal samples was isolated by applying a double bead-beating procedure in combination with the customized MaxWell® 16 Tissue LEV Total RNA Purification Kit (XAS1220; Promega Biotech AB, Stockholm, Sweden). DNA isolates were quantified and purity (OD 260/280 ratio) was assessed with a DeNovix DS-11 FX+ Spectrophotometer/Fluorometer (DeNovix Inc., Wilmington, USA) combined with the Qubit® dsDNA BR Assay Kit (Invitrogen, Carlsbad, USA). DNA isolates were further processed in triplicate PCR reactions to amplify the 16S ribosomal RNA (rRNA) V4 region of each sample combined with unique barcoded sequences to identify individual samples. PCR product formation was confirmed by gel electrophoresis and after pooling triplicate PCR products they were purified using the CleanPCR kit (CleanNA, Waddinxveen, the Netherlands). A detailed description can be found in the Supplemental materials. 200 ng of each purified barcoded sample was pooled in one library and subsequently sequenced (Illumina NovaSeq 6000, paired-end 150 bp; Eurofins Genomics Europe Sequencing GmbH, Konstanz, Germany). The 16S rRNA gene sequencing raw data has been deposited in the European Nucleotide Archive under accession number PRJEB39539.

2.7. Microbiota data analysis and processing

Sequences of the 16S rRNA gene were analyzed using NG-Tax 2.0 pipeline (Poncheewin et al., 2020) with default settings. Taxonomy was assigned to the operational taxonomic units (OTUs) using the SILVA (Quast et al., 2013) 16S rRNA gene reference database release 132. Further data analysis was performed using R version 3.6.1. Using the Phyloseq package (McMurdie and Holmes, 2013) (version 1.30.0) the OTU table with the phylogenetic tree and the metadata were constructed. OTUs with a relative abundance >0.1% in one of the individual samples were included for further data analysis. Microbiome composition plots were created using the Microbiome package (version 1.8.0) (Lahti et al., 2017). Beta diversity (Bray-Curtis dissimilarities) was assessed with Phyloseq and its statistical significance with permutational multivariate analysis of variance (PERMANOVA) applying the Adonis function (999 permutations) of Vegan package (Oksanen et al., 2019) version 2.5-6. Taxa present in one of the fecal samples with a relative abundance >1% were used for correlations and differential abundance testing. Spearman's rank correlation of the relative abundance data per taxa were made, with use of the Microbiome package, with the V_{max} and SCFA values obtained in the present study, and correlations $\rho \geq 0.5$ were included. Significant correlations after false

discovery rate (FDR) correction for multiple testing were indicated (p-values were set to 0.1 or 0.05). The web-based tool Linear Discriminant Analysis (LDA) Effect Size (LEfSe) (Segata et al., 2011) was used to identify differential abundance taxa based on the relative abundance between the two assigned groups (i.e. fructoselysine metabolizers and non-metabolizers) of the fecal samples. Statistically significant differentially abundant taxa (p-value was set to 0.05 or 0.01 for the Kruskal-Wallis test) with an effect size of the logarithmic LDA score > 2.0 were included.

2.8. Data analysis of fructoselysine degradation and SCFA formation

The data for the degradation of fructoselysine with increasing fructoselysine substrate concentrations were fitted to the standard Michaelis-Menten equation:

$$V = V_{\max} * [S] / (K_m + [S])$$

with [S] being the substrate concentration (μM), V_{\max} ($\mu\text{mol/h/g feces}$) being the apparent maximum velocity and K_m (μM) being the apparent Michaelis-Menten constant. This was done using GraphPad Prism 5 Version 5.04 (2010) software (San Diego, CA, USA). The k_{cat} was determined as V_{\max}/K_m and describes the catalytic efficiency.

For comparison of SCFA and fructoselysine concentrations in these studies, statistics between the different treatment conditions were evaluated by multiple paired *t*-tests or one-way ANOVA tests followed by Tukey's post-hoc test, where a criterion of a p-value lower than 0.05 was considered to be significant using Microsoft Excel 2016 or GraphPad Prism 5 Version 5.04 (2010). Structural formulae were drawn using ChemDraw 18.0.

3. Results

3.1. Fructoselysine degradation by the human gut microbiota using pooled fecal slurries

Fructoselysine was degraded by the human gut microbiota in the pooled fecal slurry. After optimization of the incubation conditions with respect to time and the amount of fecal slurry (Fig. 2), Michaelis-Menten kinetics K_m , V_{\max} , and k_{cat} (i.e. V_{\max}/K_m) were determined for the pooled human fecal slurries. Optimized experimental conditions consisted of 5% fecal slurry with an incubation time of 60 min at which fructoselysine degradation was still linear in time and over fecal slurry concentrations (Fig. 2). Fig. 3 shows concentration-dependent fructoselysine degradation by the pooled fecal slurries. From these data a V_{\max} of $5.1 \pm 0.6 \mu\text{mol/h/g feces}$, a K_m of $88.1 \pm 28.7 \mu\text{M}$ and a k_{cat} of $58.3 \text{ mL/h/g feces}$ were derived (Table 1).

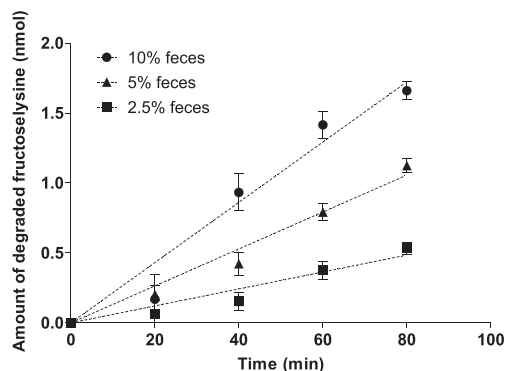


Fig. 2. Time-dependent fructoselysine ($40 \mu\text{M}$) degradation by increasing concentrations of pooled human fecal slurry. Data points show the average \pm SD from 3 repeated experiments.

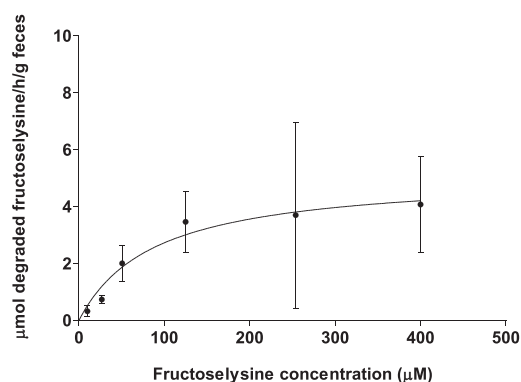


Fig. 3. Concentration-dependent degradation of fructoselysine following anaerobic incubation of fructoselysine in 5% pooled human fecal slurry over 60 min. Data points show the average \pm SD from 3 repeated experiments.

Table 1

Kinetic parameters (V_{\max} , K_m and k_{cat}) of fructoselysine degradation by the human gut microbiota of pooled and individual human fecal slurries from 16 individuals studied in vitro. Data are the average from 3 repeated experiments. NA: no or minimal activity for fructoselysine degradation, of which the kinetic parameters could not be assessed.

| Fecal slurry | V_{\max} ($\mu\text{mol/h/g feces}$) | K_m (μM) | k_{cat} (mL/h/g feces) |
|---------------|--|-------------------------|--|
| Pool | 5.1 ± 0.6 | 88.1 ± 28.7 | 58.3 |
| Individual 1 | NA | NA | NA |
| Individual 2 | 6.7 | 94.1 | 71.5 |
| Individual 3 | 7.8 | 97.0 | 80.3 |
| Individual 4 | 11.0 | 131.0 | 84.1 |
| Individual 5 | 2.7 | 20.5 | 132.7 |
| Individual 6 | 4.1 | 89.6 | 46.1 |
| Individual 7 | 6.4 | 51.4 | 124.7 |
| Individual 8 | 2.2 | 13.7 | 163.7 |
| Individual 9 | 0.8 | 20.1 | 37.5 |
| Individual 10 | NA | NA | NA |
| Individual 11 | 7.0 | 48.5 | 144.1 |
| Individual 12 | 2.0 | 53.3 | 37.9 |
| Individual 13 | NA | NA | NA |
| Individual 14 | 3.9 | 49.0 | 80.5 |
| Individual 15 | NA | NA | NA |
| Individual 16 | NA | NA | NA |

3.2. Interindividual differences in fructoselysine degradation by the human gut microbiota

Based on the results obtained for the pooled human fecal samples, kinetic parameters were determined for all 16 individual fecal slurries. Seven substrate concentrations ranging up to 5 times the K_m of the pool were used to measure the concentration-dependent degradation of fructoselysine and to derive the kinetic constants (Fig. 4, Table 1).

Fecal slurries from 5 out of the 16 individuals showed minimal to no activity towards fructoselysine degradation (i.e. individuals 1, 10, 13, 15, 16; hereafter referred to as non-metabolizers), compared to 11 out of 16 individuals where fructoselysine degradation was observed (i.e. individuals 2, 3, 4, 5, 6, 7, 8, 9, 11, 12, 14; hereafter referred to as metabolizers). For the fecal slurries from these latter 11 individuals, interindividual differences in kinetics for fructoselysine degradation were observed, with up to 14.6-fold, 9.5-fold and 4.4-fold differences in the V_{\max} , K_m and k_{cat} (i.e. V_{\max}/K_m) values, respectively. Low concentrations of baseline fructoselysine were present in fecal slurries (i.e. 1–10 μM); there was no correlation between these fructoselysine concentrations and the ability to degrade fructoselysine (Supplemental Fig. S1).

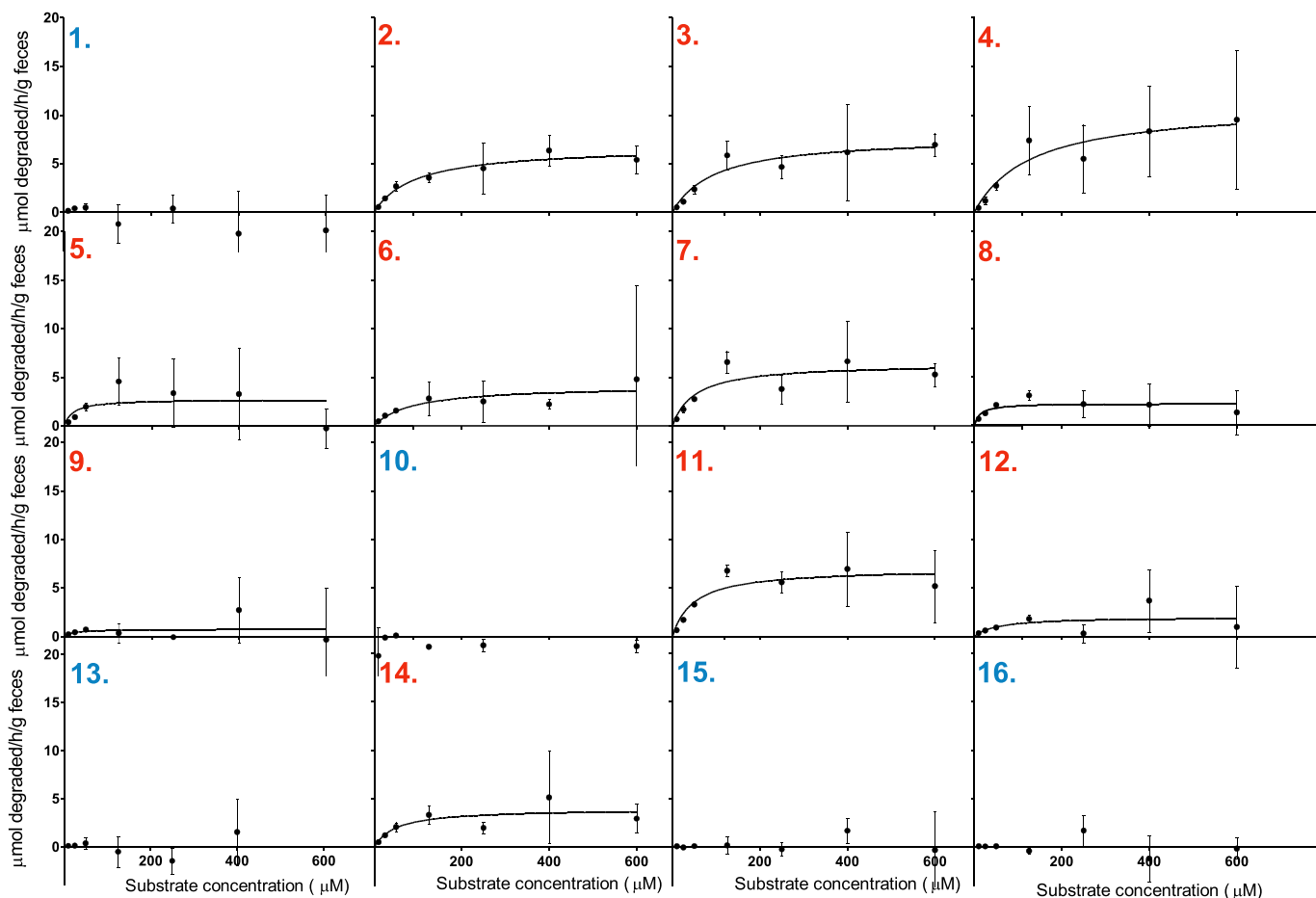


Fig. 4. Concentration-dependent degradation of fructoselysine following anaerobic incubations of 5% fecal slurries from 16 individuals (metabolizers: red; non-metabolizers: blue). Data points show the average \pm SD from 3 repeated experiments.

3.3. SCFA formation upon fructoselysine conversion by the human gut microbiota

Given that fructoselysine degradation has been described to result in SCFA formation, and predominantly butyrate (Bui et al., 2015), the changes in the levels of the SCFAs acetate, propionate and butyrate upon

incubation of fecal slurries from the 16 individuals with fructoselysine were quantified. To this end, the incubations were first optimized with pooled fecal slurries for time dependent SCFA formation in incubations with and without fructoselysine (Supplemental Fig. S2). Results obtained revealed that all three SCFAs increased in concentration over time, both in fructoselysine exposed and non-exposed fecal incubations.

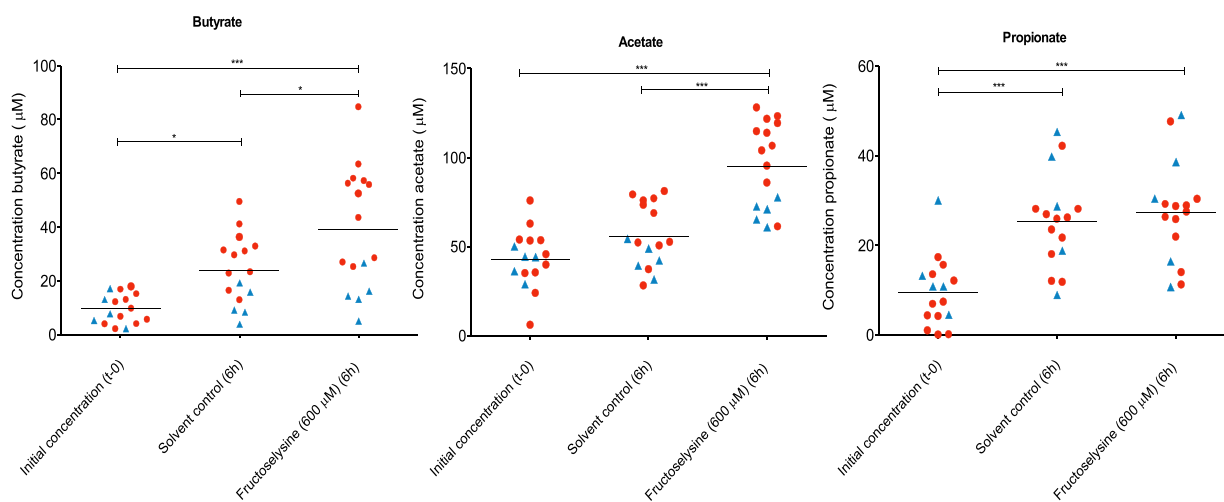


Fig. 5. Concentrations of butyrate, acetate and propionate in 5% fecal slurries of 16 human individuals at $t = 0$ and after 6 h of incubation with fructoselysine (600 μ M) or without (solvent control). Each symbol represents the data of one individual sample, averaged from 3 repeated experiments (metabolizers: red; non-metabolizers: blue). ANOVA was performed followed by Tukey's post-hoc test: * $p < 0.05$; ** $p < 0.01$; *** $p < 0.001$.

Compared to the corresponding control incubations with pooled fecal slurries without added fructoselysine, incubations with fructoselysine addition showed the largest increase in butyrate formation (1.49-fold) after 6 h incubation (Supplemental Fig. S2), and this incubation time was therefore selected for further experiments with the individual fecal slurries to quantify SCFA formation. Because SCFA formation was not assessed for linearity over time (Supplemental Fig. S2) their formation is expressed per 6 h of incubation. To allow comparison of SCFA formation between individuals, individual fecal slurries were incubated with a high concentration of fructoselysine (600 μM) to assure saturation of its degradation for all individuals (based on Fig. 4), and the concentrations of butyrate, acetate and propionate were determined. Concentrations increased in the individual fecal control incubations without fructoselysine exposure (except for acetate where 5 individuals did not show an increase) during 6 h of incubation, and addition of fructoselysine led to a significant additional increase of butyrate and acetate (Fig. 5). Inter-individual differences were observed in the concentrations of butyrate, acetate and propionate determined after 6 h of incubation in both the samples without and with added fructoselysine (Supplemental Fig. S3).

In all but one sample of the metabolizers (i.e. number 12) there was a significant fructoselysine-dependent increase in butyrate concentrations during 6 h of incubation. In 8 out of the 11 metabolizers there was as significant fructoselysine-dependent increase in acetate concentrations, and only in one of them for propionate. Only in one of the 5 non-metabolizers there was a significant fructoselysine-dependent increase in SCFA concentrations (i.e. acetate; number 15) for 6 h incubation.

Butyrate concentrations for the 11 metabolizers increased on average with $40.4 \pm 17.5 \mu\text{M}$ after exposure to fructoselysine compared to $20.0 \pm 8.5 \mu\text{M}$ in the solvent control during the 6 h of incubation. For the non-metabolizers, during the 6 h of incubation butyrate concentrations increased with $6.0 \pm 2.6 \mu\text{M}$ after exposure to fructoselysine compared to $2.2 \pm 0.7 \mu\text{M}$ in the solvent control (Supplemental Table S1).

3.4. Comparison of fructoselysine degradation and SCFA formation

To combine the results of individual fructoselysine degradation data with the formation of SCFAs, obtained V_{max} values for fructoselysine degradation were correlated to the changes in SCFA concentrations observed upon incubation with fructoselysine corrected for the level of formation in the corresponding non-exposed incubations. The fructoselysine dependent increases in SCFA concentrations were transformed to a comparable unit as used for fructoselysine degradation ($\mu\text{mol formed}/6 \text{ h/g feces}$). Linear regression revealed that fructoselysine degradation is predominantly associated with butyrate formation ($R^2 = 0.762$; Fig. 6), and to a lesser extent with acetate ($R^2 = 0.236$) and propionate formation ($R^2 = 0.006$). Based on the slope of these correlations it can be inferred that on average per 1 mol of fructoselysine

degraded per hour about 0.24 mol of butyrate is present in the incubation sample after 6 h of incubation.

3.5. Taxonomic profiling of the human fecal samples and its association with fructoselysine degradation and SCFA formation

To assess if the observed interindividual differences in fructoselysine degradation and SCFA formation are associated with bacterial composition, fecal samples were characterized using 16S rRNA gene sequencing. This analysis revealed that the individual fecal samples differed in the relative abundance of the top 10 taxa present at phylum and family level (Supplemental Fig. S4). To compare the bacterial composition of metabolizers with non-metabolizers, Bray-Curtis β -diversity was assessed and showed differences in bacterial composition between samples (Fig. 7). As shown in Fig. 7, metabolizers and non-metabolizers did not form two clear, separate clusters. However, PERMANOVA analysis of the centroids of the two groups revealed a significant difference between metabolizers and non-metabolizers (p -value < 0.01), suggesting that differences in bacterial composition between the two groups do exist, which was investigated further by differential abundance testing. This was performed by applying LEfSe. Taxa that differed significantly between metabolizers and non-metabolizers with an effect size of the logarithmic LDA score > 2.0 were identified. This

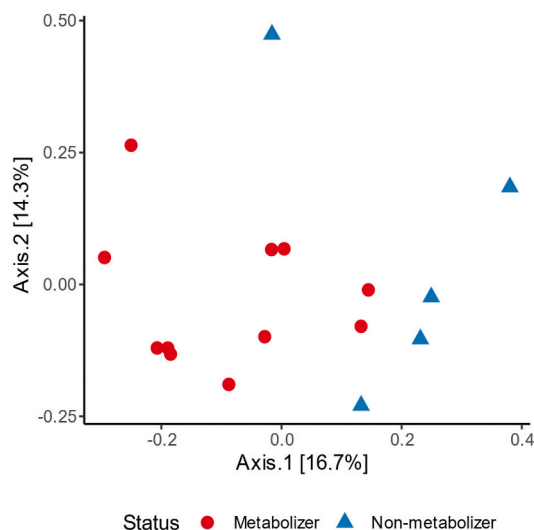


Fig. 7. Beta diversity PCoA plot of Bray-Curtis dissimilarities of the 16 human fecal samples, divided in metabolizers (red circles) and non-metabolizers (blue triangles) based on experimentally obtained V_{max} values of fructoselysine degradation.

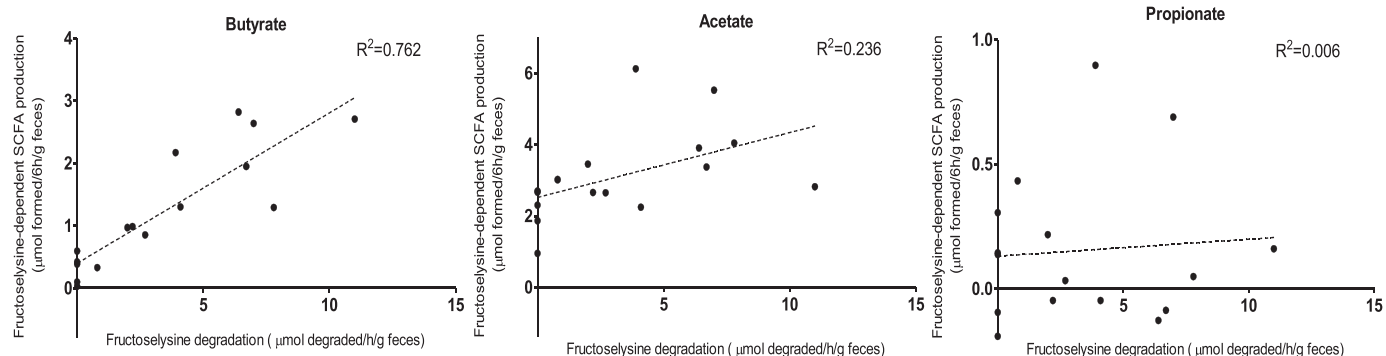


Fig. 6. Correlation of the V_{max} for fructoselysine degradation ($\mu\text{mol degraded}/\text{h/g feces}$) and fructoselysine dependent SCFA formation corrected for the level of formation in the corresponding incubations performed without added fructoselysine determined at $t = 6 \text{ h}$ ($\mu\text{mol formed}/6 \text{ h/g feces}$), experimentally obtained using fecal slurries from 16 human individuals. For samples for which no fructoselysine degradation was observed, the V_{max} for fructoselysine degradation was set at 0.

revealed 15 genera of 9 families that differed significantly (p -value < 0.05) between the two groups (Fig. 8). Three genera (*Ruminococcus_1*, *Christensenellaceae_R7_group*, *Ruminococcaceae_UCG_002*) and one family (*Christensenellaceae*) had a p -value below 0.01. These were all present in a relative abundance of on average 1–1.8% in the metabolizers and 0–0.1% in the non-metabolizers. These ratios and quantified average relative abundances for metabolizers and non-metabolizers were found to be comparable for the identified taxa *Alistipes*, *Lachnospiraceae_ND3007_group*, *Akkermansia* and *Rikenellaceae*. The significantly different family *Ruminococcaceae* was highly abundant with an average relative abundance of 24% in the metabolizers and 14% in the non-metabolizers. The significantly different family *Veillonellaceae* had an average relative abundance of 2.5% in the metabolizers versus 6% in the non-metabolizers. The significantly different phylum Proteobacteria was present with an average relative abundance of 1.2% in the metabolizers versus 2% in the non-metabolizers, while other phyla (e.g. Firmicutes, Bacteroidetes) were not significantly different between the two groups.

To identify possible relations between the relative abundance of taxa and the experimentally obtained V_{max} of fructoselysine degradation or the fructoselysine-dependent SCFA production, Spearman's rank correlation was performed. In Fig. 9 taxa correlating with one or more of the parameters with $\rho \geq 0.5$ are shown. Taxa which were also identified by LEfSe analysis were labelled grey. Several taxa were found to have a correlation with one or more parameters. For example, the relative abundance of the genus *Ruminococcus_1* was correlated to V_{max} with $\rho = 0.81$ and butyrate formation with $\rho = 0.80$. The correlation was weaker with acetate formation ($\rho = 0.57$) and not observed for propionate ($\rho = 0.19$) formation. In addition, *Lachnospiraceae_NK4A136_group*, *[Eubacterium] eligens_group*, *[Eubacterium] coprostanoligenes_group*, *Barnesiella*,

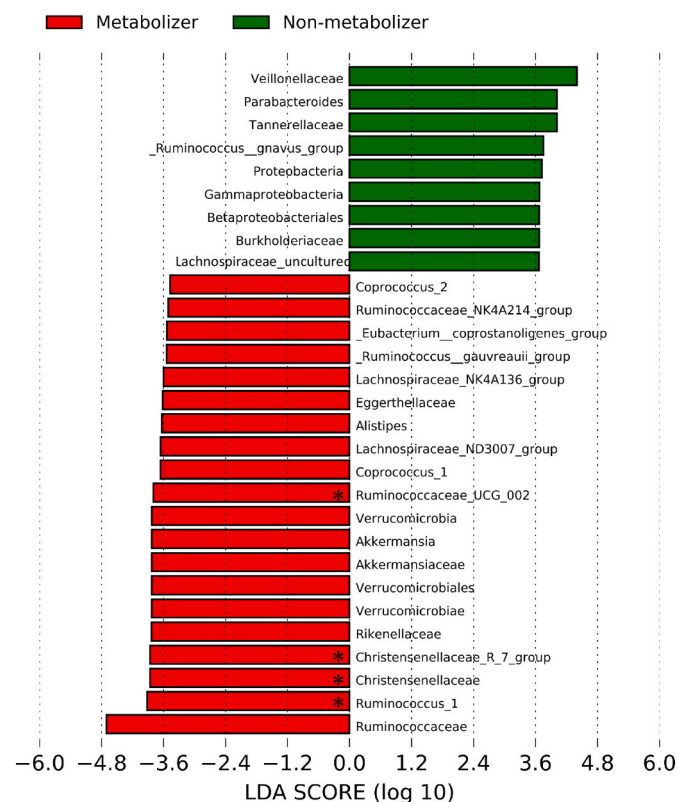


Fig. 8. LEfSe results of the significant different taxa found by comparing the metabolizers (red) with the non-metabolizers (green), ranked to their effect size. Nomenclature is based on the highest achievable taxonomic resolution level. The log10 LDA score threshold was set to 2.0 and the alpha value was set to 0.05. The taxa which remained significantly different by lowering the alpha value to 0.01 are marked (*).

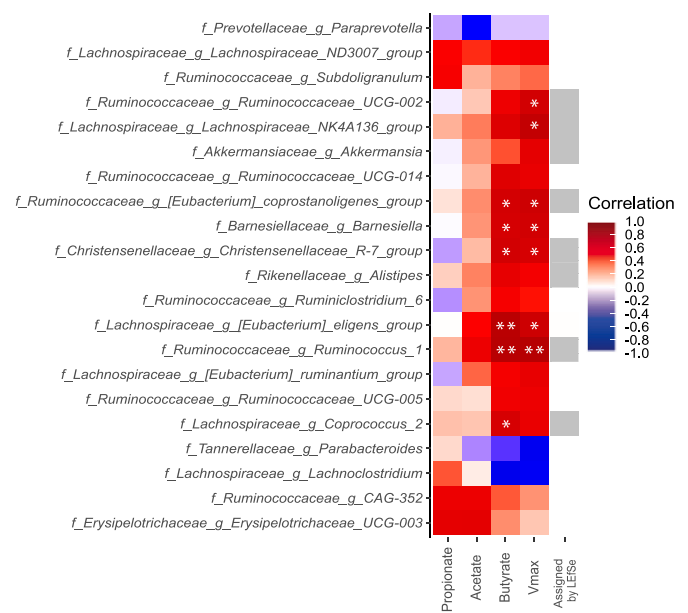


Fig. 9. Taxa correlating with the metadata (V_{max} , butyrate, acetate or propionate) of each individual (Spearman's rank correlation). Taxa with $\rho \geq 0.5$ for one or more parameters (V_{max} , butyrate, acetate or propionate) are shown. Statistically significant correlations after FDR correction are marked (* if p -values < 0.1 ; ** if p -value < 0.05). The intensity of the color corresponds to the correlation coefficient. Taxa also identified by LEfSe analysis are indicated with a grey box.

Ruminococcaceae_UCG-002 and *Christensenellaceae_R-7_group* were found to have a correlation with both the V_{max} for fructoselysine degradation ($\rho = 0.67$ to 0.75), and butyrate formation ($\rho = 0.57$ to 0.79), but only a slight or no correlation with acetate formation ($\rho = 0.15$ to 0.51) and propionate formation ($\rho = -0.22$ to 0.20). This observation of a higher correlation with butyrate than with acetate or propionate formation is in line with the observed correlations between fructoselysine degradation (V_{max} values) and SCFA production shown in Fig. 6, which revealed butyrate as the predominant SCFA formed upon fructoselysine degradation.

3.6. Interindividual differences in SCFA levels in human fecal samples

Quantified initial concentrations of SCFAs in the fecal samples, scaled up from measurements in the diluted fecal slurries (Supplemental Fig. S5), differed remarkably between individuals. It was assessed if the initial SCFA concentrations are predictive for the fructoselysine-dependent or -independent SCFA formation in incubations. Correlations of the initial SCFA concentrations with the produced SCFA concentrations revealed that initial SCFA concentrations are not associated with ($R^2 < 0.15$) and thus not predictive for fructoselysine-dependent or fructoselysine-independent SCFA formation in the fecal slurry incubations (Supplemental Fig. S6).

4. Discussion

In this study, human gut microbial degradation of fructoselysine and accompanying formation of SCFAs were quantified in vitro using anaerobic fecal incubations, which enabled the characterization of interindividual differences in this metabolic process. In line with previous observations, fructoselysine degradation in human fecal slurries was observed (Hellwig et al., 2015). Optimization of the incubation conditions to define linear conditions in time and with the amount of fecal slurry enabled definition of the kinetic parameters of this degradation, both of the pooled and individual human fecal slurries. Substantial differences in fructoselysine degradation were observed

between individuals, and non-metabolizers and metabolizers of fructoselysine could be identified. V_{\max} and K_m values for fructoselysine degradation varied up to 14.6-fold and 9.5-fold, respectively, in the group of metabolizers. Fecal samples from 5 of the 16 individuals (i.e. 31.3%; the non-metabolizers) appeared to be unable to degrade fructoselysine. In the current study, there was no association between the amount of fructoselysine already present in feces and the ability to metabolize fructoselysine, perhaps because this first characteristic is obviously also dependent on actual fructoselysine intake, which was not assessed in this study.

For the first time, we quantified Michaelis-Menten kinetics and interindividual differences of fructoselysine degradation by the human gut microbiota, using human fecal slurries. The results can be compared to data reported by Bui et al. (2015) on interindividual differences in the presence of microbiota derived genes considered relevant for this degradation (Bui et al., 2015). It was reported that only $\pm 10\%$ of the human intestinal microbial metagenomes of 65 subjects analyzed in the Human Microbiome Project (Huttenhower et al., 2012) are equipped with genes from *I. butyriciproducens* AF211 shown to be involved in fructoselysine degradation (Bui et al., 2015). The fact that the percentage of individuals in the present study able to degrade fructoselysine was substantially higher than 1–2 out of 16 indicates that also other genes, metabolic pathways, and/or microorganisms are likely to be involved in the degradation. So far, few other bacterial strains (i.e. *B. subtilis* and *E. coli*) next to *I. butyriciproducens* AF211 were shown to (partially) degrade fructoselysine (Wiame et al., 2004, 2002). However, in this study, application of 16S rRNA sequencing did not identify any of these three taxa in the human fecal samples, which might be due to e.g. absence of the taxa, presence in low abundance in the fecal samples, which has been reported before for *E. coli* in healthy populations (Ishaq et al., 2017; Wang et al., 1996), or primer choice. In general, the results of the present study provide further support for the hypothesis that additional, yet unidentified bacterial strains present in the human gut are also capable or involved in fructoselysine degradation. Several taxa were found to be positively correlated with both the V_{\max} of fructoselysine degradation and fructoselysine-dependent produced butyrate formation, where *Ruminococcus_1* showed a strong correlation ($\rho \geq 0.8$) with both parameters and might be a relevant microbe for these studied reactions, as it was also assigned as a biomarker for the metabolizers in the LEfSe analysis. Species belonging to the genus *Ruminococcus_1* have been reported to ferment carbohydrates and fibers, and produce acetate and other substrates for butyrate producing species (Mohajeri et al., 2018; Ze et al., 2012). Other taxa for which their abundance was identified to correlate with individuals' V_{\max} and butyrate formation data (*Lachnospiraceae* NK4A136 group, [*Eubacterium*] *eligens* group, *Barneisiella*, *Christenellaceae* R7 group, *Coprococcus_2*, *Alistipes*) have also been associated with SCFA production and/or carbohydrate fermentation (Morotomi et al., 2008; Song et al., 2006; Vacca et al., 2020; Waters and Ley, 2019). Overall, the correlation data and LEfSe analysis suggest that fructoselysine degradation seems to be performed by multiple microorganisms which would imply facilitation by a larger, coherent diversity. This is probably also a result from cross-feeding, with involvement of a large part of the microbial community, including low-abundant taxa (Seth and Taga, 2014).

Based on the correlation of SCFA formation with fructoselysine degradation, of the three SCFAs measured, butyrate appeared to be the preferred product of fructoselysine degradation. While propionate formation showed no correlation with fructoselysine degradation, acetate formation was weakly correlated with its degradation. Despite the low correlation of fructoselysine degradation with acetate formation, acetate showed the highest increase of the three SCFAs upon incubation with fructoselysine compared to incubations without added fructoselysine. This might be due to the fact that acetate itself is an important substrate for microbial cross-feeding, and can be formed and utilized by several other metabolic pathways occurring simultaneously in the incubations (Falony et al., 2006; Seth and Taga, 2014). After the 6 h of incubation, in

the metabolizers on average 0.24 mol of butyrate were formed per mole of fructoselysine degraded per hour, based on the individuals' V_{\max} values. This is less than the 3 mol of butyrate which have been reported to be potentially produced from 1 mol of fructoselysine by *I. butyriciproducens* AF211 (Bui et al., 2015). These differences may be explained by the fact that this reported 3:1 ratio was observed for single strain incubations and a long incubation time (i.e. 7 days), compared to the fecal slurries and relatively short incubation times used in the present study. In the incubations with fecal slurries, a more diverse bacterial composition may have facilitated different metabolic pathways and swift further catabolism of SCFAs formed (Huttenhower et al., 2012). The observed alterations in SCFA levels after fructoselysine exposure in the present study are in agreement with reports of higher SCFA levels in rat feces after exposure to fructoselysine and similar compounds (Delgado-Andrade et al., 2017). It is of interest to note that there was also SCFA formation in the anaerobic fecal slurry incubations without added fructoselysine, indicating that either constituents of the fecal samples themselves or the glycerol present in the storage buffer (De Weirdt et al., 2010) provided carbon sources to support this SCFA production by the microbiota.

Given the potential hazardous aspects of fructoselysine, the most abundant Amadori product in food (Hellwig et al., 2015), and the generally perceived beneficial effects of butyrate for human host health, the degradation of fructoselysine by the human gut bacteria is proposed to be a detoxification pathway, with, as shown in the present study, significant interindividual differences. While dietary fructoselysine appears to potentially form a hazard to human health, being a key intermediate in AGE formation (i.e. carboxymethyllysine) and reported to contribute to formation of reactive α -dicarbonyls in vivo, more insight in the adverse properties of fructoselysine and AGEs present in food, and the consequences of exposure for human health is needed. The present results will facilitate the definition of internal exposure concentrations and understanding interindividual differences therein.

The optimized in vitro method defined in this study can be used for quantification and assessment of interindividual differences in the metabolic capacity of the human gut microbiota. The model provides a way to quantify individual kinetic parameters relevant to absorption, distribution, metabolism and excretion (ADME) properties and can be applied to other (foodborne) chemicals or pharmaceuticals. The resulting data can be integrated in physiologically based kinetic (PBK) models used to extrapolate in vitro data to in vivo predictions, after scaling of the fecal incubations to the entire microbial content of the gut. There is increasing awareness for the role of the intestinal microbiome in human safety and risk assessments, and a need to develop suitable models that can be incorporated in new generation toxicity testing and risk assessment moving towards the use of human-based in vitro models as alternatives to animal experimentation (Merten et al., 2020). While longer, continuous culturing techniques might be required to study the effects of foodborne chemicals on the intestinal microbiome, the described methodology is an effective and efficient way to characterize the contribution of the gut microbiome to chemical toxicokinetics. In addition, interindividual differences can be quantified as shown in the present study, which indicated substantial interindividual differences in fructoselysine degradation and accompanying SCFA formation. This highlights the large interindividual differences present in the metabolic capacity of the human gut microbiota which can affect ADME properties and therewith health effects of (foodborne) chemicals in humans.

Data availability

Data is available upon request.

Declaration of Competing Interest

The authors declare that they have no known competing financial interests or personal relationships that could have appeared to influence

the work reported in this paper.

Acknowledgements

Research presented in this article was financially supported by the Graduate School VLAG and by the Dutch Ministry of Agriculture, Nature and Food Quality (project: KB-23-002-036). Diana M. Mendez-Catala and Qianrui Wang are acknowledged for their help with collection of the human fecal samples.

Appendix A. Supplementary data

Supplementary data to this article can be found online at <https://doi.org/10.1016/j.tiv.2021.105078>.

References

- Ahmed, M.U., Thorpe, S.R., Baynes, J.W., 1986. Identification of N epsilon-carboxymethyllysine as a degradation product of fructoselysine in glycated protein. *J. Biol. Chem.* 261, 19.
- den Besten, G., van Eunen, K., Groen, A.K., Venema, K., Reijngoud, D.-J., Bakker, B.M., 2013. The role of short-chain fatty acids in the interplay between diet, gut microbiota, and host energy metabolism. *J. Lipid Res.* 54, 2325–2340. <https://doi.org/10.1194/jlr.R036012>.
- Brings, S., Fleming, T., Freichel, M., Muckenthaler, M.U., Herzog, S., Nawroth, P.P., 2017. Dicarboxyls and advanced glycation end-products in the development of diabetic complications and targets for intervention. *Int. J. Mol. Sci.* 18 <https://doi.org/10.3390/ijms18050984>.
- Bui, T.P.N., Ritari, J., Boeren, S., De Waard, P., Plugge, C.M., De Vos, W.M., 2015. Production of butyrate from lysine and the Amadori product fructoselysine by a human gut commensal. *Nat. Commun.* 6, 1–10. <https://doi.org/10.1038/ncomms10062>.
- Ciccocioppo, R., Vanoli, A., Klersy, C., Imbesi, V., Boccaccio, V., Manca, R., Betti, E., Cangemi, G.C., Strada, E., Besio, R., Rossi, A., Falcone, C., Arduzzone, S., Fociani, P., Danelli, P., Corazza, G.R., 2013. Role of the advanced glycation end products receptor in Crohn's disease inflammation. *World J. Gastroenterol.* 19, 8269–8281. <https://doi.org/10.3748/wjg.v19.i45.8269>.
- De Weirtd, R., Possemiers, S., Vermeulen, G., Moerdijk-Poortvliet, T.C.W., Boschker, H.T. S., Verstraete, W., Van de Wiele, T., 2010. Human faecal microbiota display variable patterns of glycerol metabolism. *FEMS Microbiol. Ecol.* 74, 601–611. <https://doi.org/10.1111/j.1574-6941.2010.00974.x>.
- Delgado-Andrade, C., Fogliano, V., 2018. Dietary advanced glycosylation end-products (dAGEs) and melanoidins formed through the maillard reaction: physiological consequences of their intake. *Annu. Rev. Food Sci. Technol.* 9, 271–291. <https://doi.org/10.1146/annurev-food-030117>.
- Delgado-Andrade, C., Pastoriza de la Cueva, S., Peinado, M.J., Rufián-Henares, J.Á., Navarro, M.P., Rubio, L.A., 2017. Modifications in bacterial groups and short chain fatty acid production in the gut of healthy adult rats after long-term consumption of dietary Maillard reaction products. *Food Res. Int.* 100, 134–142. <https://doi.org/10.1016/j.foodres.2017.06.067>.
- Erbarsdobl, H.F., Faist, V., 2001. Metabolic transit of Amadori products. *Nahrung/Food* 45, 177–181. [https://doi.org/10.1002/1521-3803\(20010601\)45:3<177::AID-FOOD177>3.0.CO;2-A](https://doi.org/10.1002/1521-3803(20010601)45:3<177::AID-FOOD177>3.0.CO;2-A).
- Erbarsdobl, H.F., Somoza, V., 2007. Forty years of furosine – forty years of using Maillard reaction products as indicators of the nutritional quality of foods. *Mol. Nutr. Food Res.* 51, 423–430. <https://doi.org/10.1002/mnfr.200600154>.
- Falony, G., Vlachou, A., Verbrugghe, K., De Vuyst, L., 2006. Cross-feeding between *Bifidobacterium longum* BB536 and acetate-converting, butyrate-producing colon bacteria during growth on oligofructose. *Appl. Environ. Microbiol.* 72, 7835–7841. <https://doi.org/10.1128/AEM.01296-06>.
- Grunwald, S., Krause, R., Bruch, M., Henle, T., Brandsch, M., 2006. Transepithelial flux of early and advanced glycation compounds across Caco-2 cell monolayers and their interaction with intestinal amino acid and peptide transport systems. *Br. J. Nutr.* 95, 1221–1228. <https://doi.org/10.1079/BJN20061793>.
- Hamer, H.M., Jonkers, D., Venema, K., Vanhoutvin, S., Troost, F.J., Brummer, R.-J., 2007. The role of butyrate on colonic function. *Aliment. Pharmacol. Ther.* 27, 104–119. <https://doi.org/10.1111/j.1365-2036.2007.03562.x>.
- Han, J., Lin, K., Sequeira, C., Borchers, C.H., 2015. An isotope-labeled chemical derivatization method for the quantitation of short-chain fatty acids in human feces by liquid chromatography–tandem mass spectrometry. *Anal. Chim. Acta* 854, 86–94. <https://doi.org/10.1016/j.aca.2014.11.015>.
- Hellwig, M., Geissler, S., Matthes, R., Peto, A., Silow, C., Brandsch, M., Henle, T., 2011. Transport of free and peptide-bound glycated amino acids: synthesis, transepithelial flux at Caco-2 cell monolayers, and interaction with apical membrane transport proteins. *ChemBioChem* 12, 1270–1279. <https://doi.org/10.1002/cbic.2011000759>.
- Hellwig, M., Bunzel, D., Huch, M., Franz, C.M.A.P., Kulling, S.E., Henle, T., 2015. Stability of individual maillard reaction products in the presence of the human colonic microbiota. *J. Agric. Food Chem.* 63, 6723–6730. <https://doi.org/10.1021/acs.jafc.5b01391>.
- Henle, T., 2005. Protein-bound advanced glycation endproducts (AGEs) as bioactive amino acid derivatives in foods review article. *Amino Acids* 29, 313–322. <https://doi.org/10.1007/s00726-005-0200-2>.
- Huttenhower, C., Gevers, D., Knight, R., et al., 2012. Structure, function and diversity of the healthy human microbiome. *Nature* 486, 207–214. <https://doi.org/10.1038/nature11234>.
- Ishaq, H.M., Mohammad, I.S., Guo, H., Shahzad, M., Hou, Y.J., Ma, C., Naseem, Z., Wu, X., Shi, P., Xu, J., 2017. Molecular estimation of alteration in intestinal microbial composition in Hashimoto's thyroiditis patients. *Biomed. Pharmacother.* 95, 865–874. <https://doi.org/10.1016/j.biopha.2017.08.101>.
- Kellow, N.J., Coughlan, M.T., 2015. Effect of diet-derived advanced glycation end products on inflammation. *Nutr. Rev.* 73, 737–759. <https://doi.org/10.1093/nutrit/nuv030>.
- Kislinger, T., Fu, C., Huber, B., Qu, W., Taguchi, A., Du Yan, S., Hofmann, M., Yan, S.F., Pischetsrieder, M., Stern, D., Schmidt, A.M., 1999. N(epsilon)-(carboxymethyl)lysine adducts of proteins are ligands for receptor for advanced glycation end products that activate cell signaling pathways and modulate gene expression. *J. Biol. Chem.* 274, 31740–31749. <https://doi.org/10.1074/jbc.274.44.31740>.
- Koschinsky, T., He, C.-J., Mitsuhashi, T., Bucala, R., Liu, C., Buenting, C., Heitmann, K., Vlassara, H., 1997. Orally absorbed reactive glycation products (glycotoxins): an environmental risk factor in diabetic nephropathy. *Proc. Natl. Acad. Sci.* 94, 6474–6479. <https://doi.org/10.1073/pnas.94.12.6474>.
- Lahti, L., Shetty, S.A., et al., 2017. Tools for Microbiome Analysis in R [WWW Document]. <http://microbiome.github.com/microbiome>. URL: <http://microbiome.github.com/microbiome> (accessed 6.15.20).
- Lee, K., Erbersdobl, H.F., 2005. Balance experiments on human volunteers with epsilon-fructoselysine (FL) and lysinoalanine (LAL). *Mail. React. Chem. Food Heal.* 358–363. <https://doi.org/10.1533/9781845698393.4.358>.
- Li, M., Zeng, M., He, Z., Zheng, Z., Qin, F., Tao, G., Zhang, S., Chen, J., 2015. Increased accumulation of protein-bound N epsilon-(carboxymethyl)lysine in tissues of healthy rats after chronic Oral N epsilon-(carboxymethyl)lysine. *J. Agric. Food Chem.* 63, 1658–1663. <https://doi.org/10.1021/jf505063t>.
- Liang, Z., Chen, X., Li, L., Li, B., Yang, Z., 2019. The fate of dietary advanced glycation end products in the body: from oral intake to excretion. *Crit. Rev. Food Sci. Nutr.* <https://doi.org/10.1080/10408398.2019.1693958>.
- Liu, X., Zheng, L., Zhang, R., Liu, G., Xiao, S., Qiao, X., Wu, Y., Gong, Z., 2016. Toxicological evaluation of advanced glycation end product N(epsilon)-(carboxymethyl) lysine: acute and subacute oral toxicity studies. *Regul. Toxicol. Pharmacol.* 77, 65–74. <https://doi.org/10.1016/j.yrtph.2016.02.013>.
- Mcmurdie, P.J., Holmes, S., 2013. Phyloseq: an R package for reproducible interactive analysis and graphics of microbiome census data. *PLoS One* 8, e61217. <https://doi.org/10.1371/journal.pone.0061217>.
- Mehta, B.M., Deeth, H.C., 2016. Blocked lysine in dairy products: formation, occurrence, analysis, and nutritional implications. *Compr. Rev. Food Sci. Food Saf.* 15, 206–218. <https://doi.org/10.1111/1541-4337.12178>.
- Merten, C., Schoonjans, R., Di Gioia, D., Peláez, C., Sanz, Y., Maurici, D., Robinson, T., 2020. Editorial: Exploring the need to include microbiomes into EFSA's scientific assessments. *EFSA J.* 18. <https://doi.org/10.2903/j.efsa.2020.e18061>.
- Mohajeri, M.H., Brummer, R.J.M., Rastall, R.A., Weersma, R.K., Harmsen, H.J.M., Faas, M., Eggerdörfer, M., 2018. The role of the microbiome for human health: from basic science to clinical applications. *Eur. J. Nutr.* 57, 1–14. <https://doi.org/10.1007/s00394-018-1703-4>.
- Morotomi, M., Nagai, F., Sakon, H., Tanaka, R., 2008. *Dialister succinatiphilus* sp. nov. and *Barnesiella intestinihominis* sp. nov., isolated from human faeces. *Int. J. Syst. Evol. Microbiol.* 58, 2716–2720. <https://doi.org/10.1099/IJS.0.2008/000810-0>.
- Nicholson, J.K., Holmes, E., Kinross, J., Burcelin, R., Gibson, G., Jia, W., Pettersson, S., 2012. Host-gut microbiota metabolic interactions. *Science* 336, 1262–1267. <https://doi.org/10.1126/science.1223813>.
- Oksanen, J., Guillaume, B., Friendly, M., Kindt, R., Legendre, P., McGinn, D., Minchin, P. R., O'Hara, R.B., Simpson, G.L., Solymos, P., Stevens, M.H.H., Szoecs, E., Wagner, H., 2019. *vegan: Community Ecology Package*. R Package Version 2.5-6 [WWW document]. <https://cran.r-project.org/package=vegan> (accessed 6.15.20).
- Poncheewin, W., Hermes, G.D.A., van Dam, J.C.J., Koehorst, J.J., Smidt, H., Schaap, P.J., 2020. NG-tax 2.0: a semantic framework for high-throughput amplicon analysis. *Front. Genet.* 10 <https://doi.org/10.3389/fgene.2019.01366>.
- Poulsen, M.W., Hedegaard, R.V., Andersen, J.M., de Courten, B., Bügel, S., Nielsen, J., Skibsted, L.H., Dragsted, L.O., 2013. Advanced glycation endproducts in food and their effects on health. *Food Chem. Toxicol.* 60, 10–37. <https://doi.org/10.1016/j.fct.2013.06.052>.
- Quast, C., Pruesse, E., Yilmaz, P., Gerken, J., Schweer, T., Yarza, P., Peplies, J., Glöckner, F.O., 2013. The SILVA ribosomal RNA gene database project: improved data processing and web-based tools. *Nucleic Acids Res.* 41, D590–D596. <https://doi.org/10.1093/nar/gks1219>.
- Scheijen, J.L.J.M., Hanssen, N.M.J., van Greevenbroek, M.M., Van der Kallen, C.J., Feskens, E.J.M., Stehouwer, C.D.A., Schalkwijk, C.G., 2018. Dietary intake of advanced glycation endproducts is associated with higher levels of advanced glycation endproducts in plasma and urine: the CODAM study. *Clin. Nutr.* 37, 919–925. <https://doi.org/10.1016/j.clnu.2017.03.019>.
- Segata, N., Izard, J., Waldron, L., Gevers, D., Miropolsky, L., Garrett, W.S., Huttenhower, C., 2011. Metagenomic biomarker discovery and explanation. *Genome Biol.* 12, R60. <https://doi.org/10.1186/gb-2011-12-6-r60>.
- Sergi, D., Boulestijn, H., Campbell, F.M., Williams, L.M., 2020. The role of dietary advanced glycation end products in metabolic dysfunction. *Mol. Nutr. Food Res.* 1900934. <https://doi.org/10.1002/mnfr.201900934>.
- Seth, E.C., Taga, M.E., 2014. Nutrient cross-feeding in the microbial world. *Front. Microbiol.* 5, 350. <https://doi.org/10.3389/fmicb.2014.00350>.

- Snelson, M., Coughlan, M.T., 2019. Dietary advanced glycation end products: digestion, metabolism and modulation of gut microbial ecology. *Nutrients*. <https://doi.org/10.3390/nu11020215>.
- Somoza, V., Wenzel, E., Weiß, C., Clawin-Rädecker, I., Grübel, N., Erbersdobler, H.F., 2006. Dose-dependent utilisation of casein-linked lysinoalanine, N(epsilon)-fructoselysine and N(epsilon)-carboxymethyllysine in rats. *Mol. Nutr. Food Res.* 50, 833–841. <https://doi.org/10.1002/mnfr.200600021>.
- Song, Y., Könönen, E., Rautio, M., Liu, C., Bryk, A., Eerola, E., Finegold, S.M., 2006. *Alistipes onderdonkii* sp. nov. and *Alistipes shahii* sp. nov., of human origin. *Int. J. Syst. Evol. Microbiol.* 56, 1985–1990. <https://doi.org/10.1099/ijs.0.64318-0>.
- Uribarri, J., Cai, W., Sandu, O., Peppas, M., Goldberg, T., Vlassara, H., 2005. Diet-derived advanced glycation end products are major contributors to the body's AGE pool and induce inflammation in healthy subjects. *Ann. N. Y. Acad. Sci.* 1043, 461–466. <https://doi.org/10.1196/annals.1333.052>.
- Vacca, M., Celano, G., Calabrese, F.M., Portincasa, P., Gobetti, M., De Angelis, M., 2020. The controversial role of human gut lachnospiraceae. *Microorganisms* 8, 573. <https://doi.org/10.3390/microorganisms8040573>.
- Van Nguyen, C., 2006. Toxicity of the AGEs generated from the Maillard reaction: on the relationship of food-AGEs and biological-AGEs. *Mol. Nutr. Food Res.* 50, 1140–1149. <https://doi.org/10.1002/mnfr.200600144>.
- Vlassara, H., Palace, M.R., 2002. Diabetes and advanced glycation endproducts. *J. Intern. Med.* 251, 87–101. <https://doi.org/10.1046/j.1365-2796.2002.00932.x>.
- Wang, R.-F., Cao, W.-W., Cerniglia, C.E., 1996. PCR detection and quantitation of predominant anaerobic bacteria in human and animal fecal samples. *Appl. Environ. Microbiol.* 62, 1242–1247.
- Waters, J.L., Ley, R.E., 2019. The human gut bacteria Christensenellaceae are widespread, heritable, and associated with health. *BMC Biol.* <https://doi.org/10.1186/s12915-019-0699-4>.
- Wiame, E., Delpierre, G., Collard, F., Van Schaftingen, E., 2002. Identification of a pathway for the utilization of the Amadori product fructoselysine in *Escherichia coli*. *J. Biol. Chem.* 277, 42523–42529. <https://doi.org/10.1074/jbc.M200863200>.
- Wiame, E., Duquenne, A., Delpierre, G., Van Schaftingen, E., 2004. Identification of enzymes acting on α -glycated amino acids in *Bacillus subtilis*. *FEBS Lett.* 577, 469–472. <https://doi.org/10.1016/j.febslet.2004.10.049>.
- Xue, J., Rai, V., Singer, D., Chabierski, S., Xie, J., Reverdatto, S., Burz, D.S., Schmidt, A. M., Hoffmann, R., Shekhtman, A., 2011. Advanced glycation end product recognition by the receptor for AGEs. *Structure* 19, 722–732. <https://doi.org/10.1016/j.str.2011.02.013>.
- Yaylayan, V.A., Huyghues-Despointes, A., Feather, M.S., 1994. Chemistry of Amadori rearrangement products: analysis, synthesis, kinetics, reactions, and spectroscopic properties. *Crit. Rev. Food Sci. Nutr.* 34, 321–369. <https://doi.org/10.1080/10408399409527667>.
- Ze, X., Duncan, S.H., Louis, P., Flint, H.J., 2012. *Ruminococcus bromii* is a keystone species for the degradation of resistant starch in the human colon. *ISME J.* 6, 1535–1543. <https://doi.org/10.1038/ismej.2012.4>.
- Zhao, D., Sheng, B., Wu, Y., Li, H., Xu, D., Nian, Y., Mao, S., Li, C., Xu, X., Zhou, G., 2019. Comparison of free and bound advanced glycation end products in food: a review on the possible influence on human health. *J. Agric. Food Chem.* 67, 14007–14018. <https://doi.org/10.1021/acs.jafc.9b05891>.